OPEN ACCESS

Saudi Journal of Engineering and Technology
Abbreviated Key Title: Saudi J Eng Technol
ISSN 2415-6272 (Print) | ISSN 2415-6264 (Online)
Scholars Middle East Publishers, Dubai, United Arab Emirates
Journal homepage: https://saudijournals.com

Original Research Article

Prediction and Optimization of Cutting Forces required to Minimize Tool Breakage during Dry Drilling Operations

Onyiriuka F. O.[1*], Mohammed B. A.[2], Onwuamaeze I. P.[2]

[1]Department of Production Engineering, University of Benin, Benin City, +234, Nigeria
[2]Department of Mechanical Engineering, Petroleum Training Institute, Effurun, +234, Nigeria

DOI: 10.36348/sjet.2024.v09i03.006 | **Received:** 06.02.2024 | **Accepted:** 11.03.2024 | **Published:** 14.03.2024

***Corresponding author:** Onyiruika F. O.
Department of Production Engineering, University of Benin, Benin City, +234, Nigeria

Abstract

Drilling is one of the most common and rudimental machining methods in the manufacturing industries for removal of unwanted material from the workpiece. How the cutting instrument and workpiece interact results in a mechanical force that causes the formation of chips during penetration, and these chips are evacuated through the flute created on the body of the drill tool. The interplay of forces at the drill point generates high temperatures, needed for the physical and chemical processes that weaken tools and lead to breakage. Optimal experimental designs are very important to obtain accurate optimization of engineering processes, an expert method was used to design the experimental layout and utilizing the Design Expert software, an experimental matrix which developed the parameters design of twenty experimental runs. The present study uses Artificial Neural Networks (ANN) and Response Surface Methodology (RSM) to forecast and optimize cutting forces during dry drilling operations. In developing the model, a dataset that included several factors such as depth of cut, feed rate, and cutting speed was used. The RSM model demonstrated a significant correlation between input parameters and cutting forces, as evidenced by its high coefficient of determination (R^2) of 0.9493. On the other hand, the ANN model, which was trained using 70% of the data and validated using 15% of the data, showed a little lower R^2 value of 0.81434, but it was still able to make accurate predictions. Cutting forces were well predicted by both models, with RSM exhibiting a somewhat better performance in terms of accuracy. The results indicate that both RSM and ANN can be useful instruments for dry drilling cutting force optimization, offering insights for increased productivity and efficiency in machining operations.

Keywords: cutting forces, dry drilling, response surface methodology, artificial neural network.

1. INTRODUCTION

The sectors involved in machining are continuously searching and finding new methods to lessen the forces produced when cutting metal, lengthen the tool's life, and better surface quality (Velan *et al.*, 2021). Workpiece deformation that is elastic and the subsurface residual stress injection that occurs during cutting can reduce the precision of machining. It is vital to have a better understanding of how cutting circumstances and tool wear affect finished surfaces and their geometrical flaws to be able to predict how cutting forces affect changes in surface integrity (Toubhans *et al.*, 2020). Cutting forces have a significant impact on tool wear, surface quality, and overall machining efficiency when doing machining processes. To increase machining operations and increase tool life, cutting force prediction and optimization are crucial (Imani *et al.*, 2020). Different materials have different machining properties, therefore specific methods for anticipating and maximizing cutting pressures are required (Gupta *et al.*, 2022). Optimizing cutting forces in practical applications frequently entails juggling competing goals like avoiding tool wear, increasing material removal rate, and lowering energy usage. To find Pareto-optimal solutions, multi-objective optimization methods such as evolutionary algorithms are applied. Foreseeing and optimizing cutting forces requires a thorough understanding of the wear mechanisms that take place during the machining process. The following wear modes exist: adhesion, abrasion, diffusion, flank wear, and crater wear. The choice of tool material has a considerable influence on tool life and cutting forces.

(Xavior & Jeyapandiarajan, 2019) In order to improve tool performance, research in this field examines the creation of improved tool materials such as ceramics, carbides, and coatings. Processes for machining optimization can be greatly aided by machine learning techniques. Increased tool life can improve the cutting process' machinability and sustainability. Cutting fluids are preferably used to extend the tool life. Nonetheless, most cutting fluids are not biodegradable by nature and have negative environmental risks (Ali *et al.*, 2022). In order to forecast three parameters for cutting used in high speed turning operations: cutting force (Fc), surface roughness (Ra), and tool lifespan (T), Zhang and Xu (2021) built Gaussian process regression models according to the cutting speed (V_c), feed rate (*f*), and depth of cut (a_p). The life and cutting force coefficients (CFCs) were established in the work by Broderick *et al.*, (2021) by evaluating the machinability performance of additives (mineraloil, phosphate ester (P-ester), and dialkyl pentasulphide). Cutting-edge micro-geometry is crucial to the process of machining. Wear resistance, tool life, and process dependability are all improved by cutting edges that are the right size and form (Lv *et al.*, 2020). When cutting CFRP materials, tool shape plays a big role (Knápek *et al.*, 2023). To increase machining precision and tool life during the power skiving process, Onozuka *et al.*, (2020) created a computational model for the cutting forces and area. Internal gear power skiving involves complicated interactions between the direction of the cut as well as the relative velocity of the device and the piece of work, chip thickness, and effective rake angle. In order to improve machined surface integrity and tool life, which was an important issue to be tackled in turning of iron-based superalloy, Zhang *et al.*, (2020) looked into the surface roughness, cutting force, and tool life. GH2132 was the subject of turning experiments using coated carbide and cermet tools. According to Karpuschewski *et al.*, (2018), the Workpiece-Fixture-Machine Tool-Cutting Tool (WFMC) system's workload and tool life are affected by the force increase. Since the cutting force can only be computed using the Kienzle and Viktor connection when utilizing a feed rate that is substantially higher than usual, we must be aware of the change in the particular cutting force (kc1.1) as well as the exponent associated with it (z). There are now new opportunities and problems in forecasting and optimizing cutting forces as a result of recent developments in machining technology, such as high-speed machining, cryogenic machining, and sustainable machining. It is a challenging and interdisciplinary area of research to predict and optimize cutting forces for increasing tool life and machining effectiveness. In addition to an understanding of material properties, tool wear mechanisms, and optimization approaches, it requires a combination of analytical, empirical, and computational methods (Kuntolu *et al.*, 2020). This field's advancements help a variety of industries' machining operations become more economical and environmentally friendly.

2. METHODOLOGY

2.1 Research Design

The present study deals with the forces that comes to play during dry drilling that can cause tool breakage, with a view of examining the their causative effects. The drilling operation will be conducted on a DT drilling machine. The information gotten from literature was used as a guide for the selection of the major steps involved in dry drilling process. A central composite design was selected, considering four main drilling variables, specifically cutting depth, feed rate, and cutting speed. The material used was mild steel plate with dimension 100mm by 400mm by 50mm, where about 100 samples was produced for this experiment.

2.2 Response Surface Methodology

In RSM, the function's optimal value might be either minimal or maximal depending on the process input parameters. It is an optimization techniques that is currently being widely utilized to assess the performance of the welding process and determine the most appropriate optimal solution of responses to the input variables. RSM is a collection of statistical and algebraic methods that are helpful in modeling and forecasting the response of interest that depends on several variables for input in order to minimize or maximize this response.

2.3 Artificial Neural Network

Neural networks are tools for data mining that are used to find patterns in databases that are hidden. There are two important ways in which they mimic the brain, functioning as massively parallel distributed processors. Through a process of learning, the network gains knowledge. Synaptic weights, another name for interneuron connection strengths, are where this information is kept. An appropriate weight, represented by the letter w, is applied to a basic neuron with R input. The input to the transfer function f is the total weighted inputs plus the bias. Any differentiable transfer function f can be utilized by neurons to generate their output. The log-sigmoid transfer function, or logsig, is widely employed in multilayer networks and generates outputs in the 0 to 1 range when the net input of the neuron varies reaching positive infinity from negative. The tan-sigmoid transfer function, or tansig, is an additional option for multilayer networks. Whereas linear output neurons are typically employed for function fitting issues, sigmoid output neurons are frequently utilized for pattern recognition tasks.

3. RESULTS AND DISCUSSION

In this investigation, twenty set of experiments was done, each experimental run comprising the depth of cut, feed rate, and cutting speed. The cutting force response were measured.

3.1 Modeling using RSM

Design of experiment and process optimization was implemented utilizing statistical software. In this

instance, Design Expert 7.01 was applied. The sequential model sum of squares was computed for the measured cutting force, as shown in Table 1, to confirm that the quadratic model was suitable for interpreting the experimental results.

Tables 1: Sequential sum of square for measured cutting force

Source	Sum of Squares	Df	Mean Square	F Value	p-value Prob > F	
Mean vs Total	1.038×10^6	1	1.038×10^6			
Linear vs Mean	55990.46	3	18663.49	2.20	0.1281	
2FI vs Linear	2940.38	3	980.13	0.096	0.9610	
Quadratic vs 2FI	1.233×10^5	3	41087.85	42.23	< 0.0001	Suggested
Cubic vs Quadratic	5788.04	4	1447.01	2.20	0.1851	Aliased
Residual	3940.78	6	656.80			
Total	1.230×10^6	20	61489.00			

From Table 1, the Quadratic vs 2FI model is suggested based on the sequential model sum of square. It was shown that the 'Cubic vs Quadratic' model is aliased, making it unfit for use.

The lack of fit test is calculated in order to determine as to what degree does the quadratic model account for the fundamental variance associated with the experimental findings. It is not possible using a model with a considerable lack of fit for prediction, hence, the calculated lack of fit results for the cutting force is illustrated in Table 2.

Table 2: Lack of fit Test for Cutting Force Response

Source	Sum of Squares	df	Mean Square	F Value	p-value Prob > F	
Linear	1.320×10^5	11	11999.39	15.23	0.0038	
2FI	1.291×10^5	8	16131.61	20.47	0.0020	
Quadratic	5789.32	5	1157.86	1.47	0.3415	Suggested
Cubic	1.28	1	1.28	1.624×10^{-3}	0.9694	Aliased
Pure Error	3939.50	5	787.90			

It was observed from Table 2, that due to a considerable lack of fit, the cubic polynomial was aliased to model analysis, whereas the non-significant lack of fit of the quadratic polynomial is suggested for the model's analysis. Table 3 shows the Model Summary Statistics calculated for the Cutting Force Response.

Table 3: Model Summary Statistics for the Cutting Force Response

Source	Std. Dev.	R-Squared	Adjusted R-Squared	Predicted R-Squared	PRESS	
Linear	92.17	0.2917	0.1589	-0.0237	1.965×10^5	
2FI	101.14	0.3071	-0.0128	-0.6905	3.244×10^5	
Quadratic	31.19	0.9493	0.9037	0.7410	49705.85	Suggested
Cubic	25.63	0.9795	0.9350	0.9690	5950.56	Aliased

Table 3 illustrates the selected Models' adjusted r-squared, predicted r-squared, predicted error sum of square (PRESS) statistic, coefficient of determination (R^2), standard deviation (Root MSE), and predicted R-squared. The cubic polynomial model is aliased while the quadratic polynomial model is recommended because it had the greatest anticipated r-square value, the smallest predicted error sum of square value, and the greatest adjusted r-square value. The goodness of fit statistics used to confirm the quadratic model suitability is shown in Table 4.

Table 4: GOF for validating Model Significance Cutting Force

Std. Dev.	31.19	R-Squared	0.9493
Mean	227.80	Adj R-Squared	0.9037
C.V. %	13.69	Pred R-Squared	0.7410
PRESS	49705.85	Adeq Precision	13.003

From Table 4, there is decent amount of agreement between the 'Adj R-Squared' value of 0.9037 and the 'Predicted R-Squared' value of 0.7410. The computed ratio of 13.003 denotes a sufficient signal.

Figure 1 showns the normal probability plot of the residual for cutting force in order to assess the response surface model statistical features.

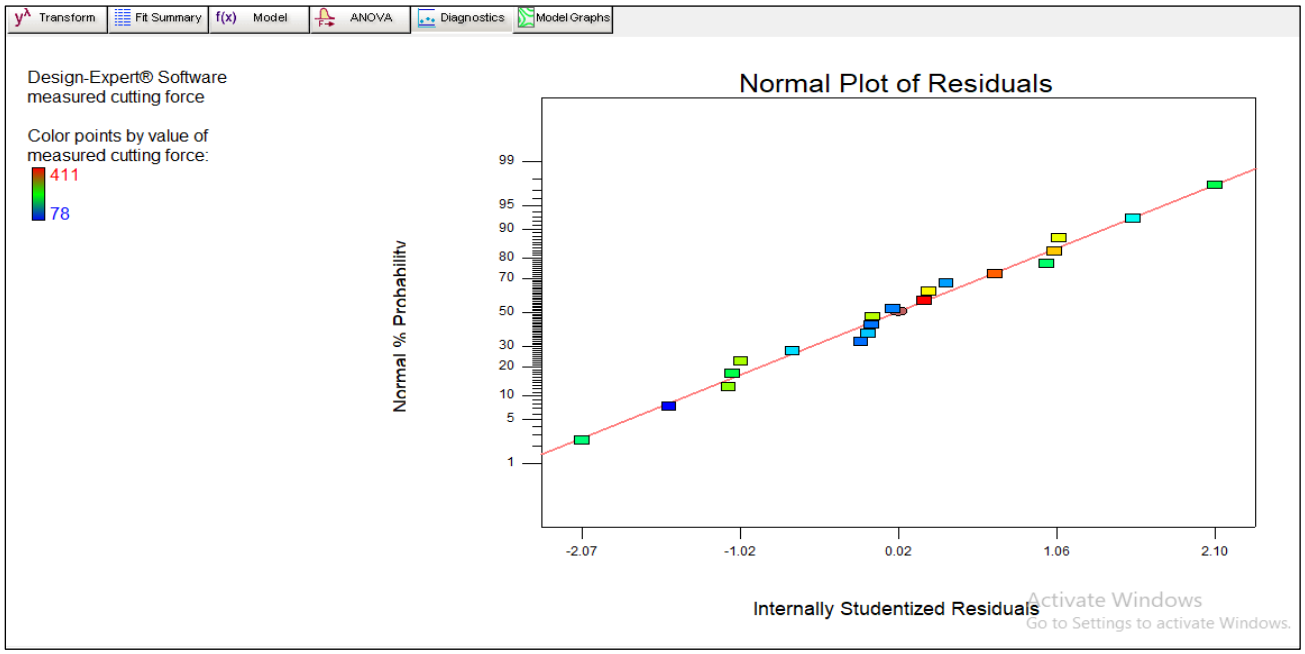

Figure 1: Normal probability plot of studentized residuals for cutting force

The normality of the computed residuals evaluated using the normal probability plot of studentized residuals. In order to determine if the residuals (observed – expected) adhere to a normal distribution, the normal probability plot of residuals, which represents the actual values' number of standard deviations is utilized.

The cook's distance indicates the amount by which the regression would change if the outlier were eliminated from the investigation. Thus, it is important to look into any point that appears to be an outlier and possesses a distance value that is significantly higher than the other points as described in Figure 2.

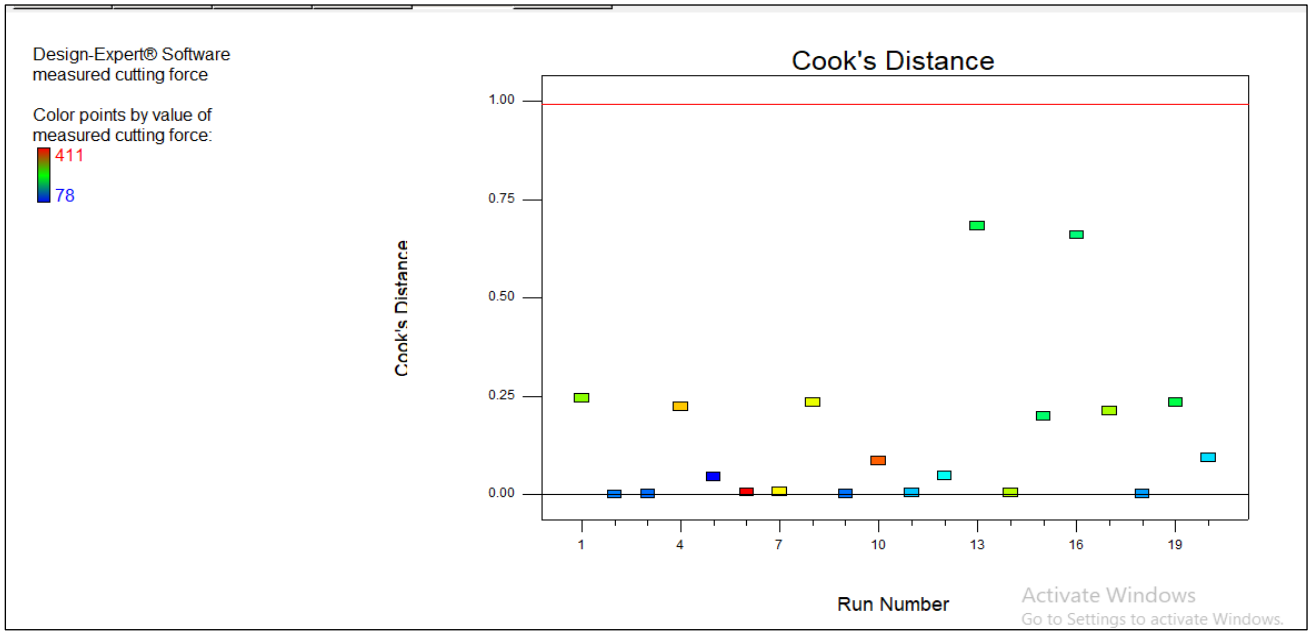

Figure 2: Generated cook's distance for cutting force

As shown in Figure 3, the cook's distance plot has an upper bound of 1.00 and a lower bound of 0.00. Experimental values that deviate significantly from the bottom or upper bounds are known as outliers and

require close examination. From Figure 3, there are no potential outliers thus, demonstrating the suitability of the experimental data.

The three-dimensional surface map shown in Figure 3, describes how the combined input factors affects the cutting force response,

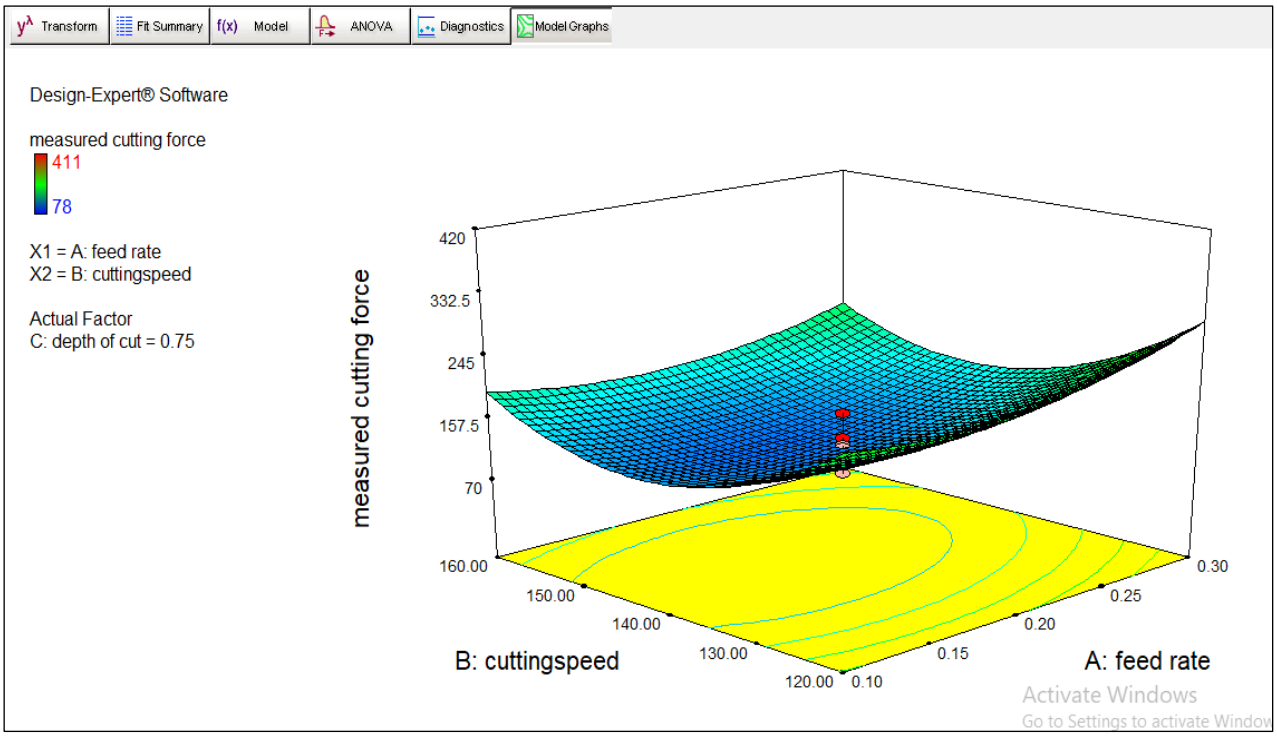

Figure 3: 3D Surface Plot for measured cutting force, cutting speed and feed rate

In Figure 4, the 3D surface plots illustrates the impacts of combining input factors on the response variable (cutting force).

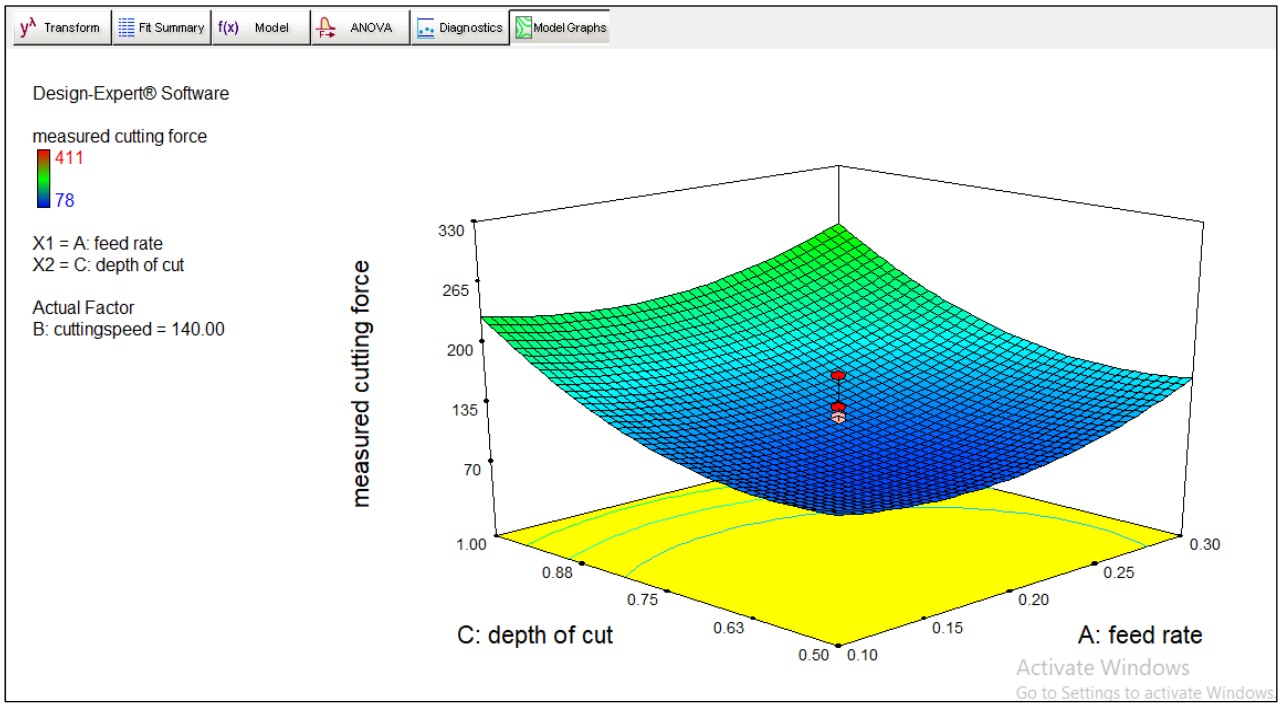

Figure 4: 3D Surface Plot for measured cutting force, depth of cut and feed rate

Figure 5 displays the 3D surface plots by combining input factors affects the response variable, cutting force.

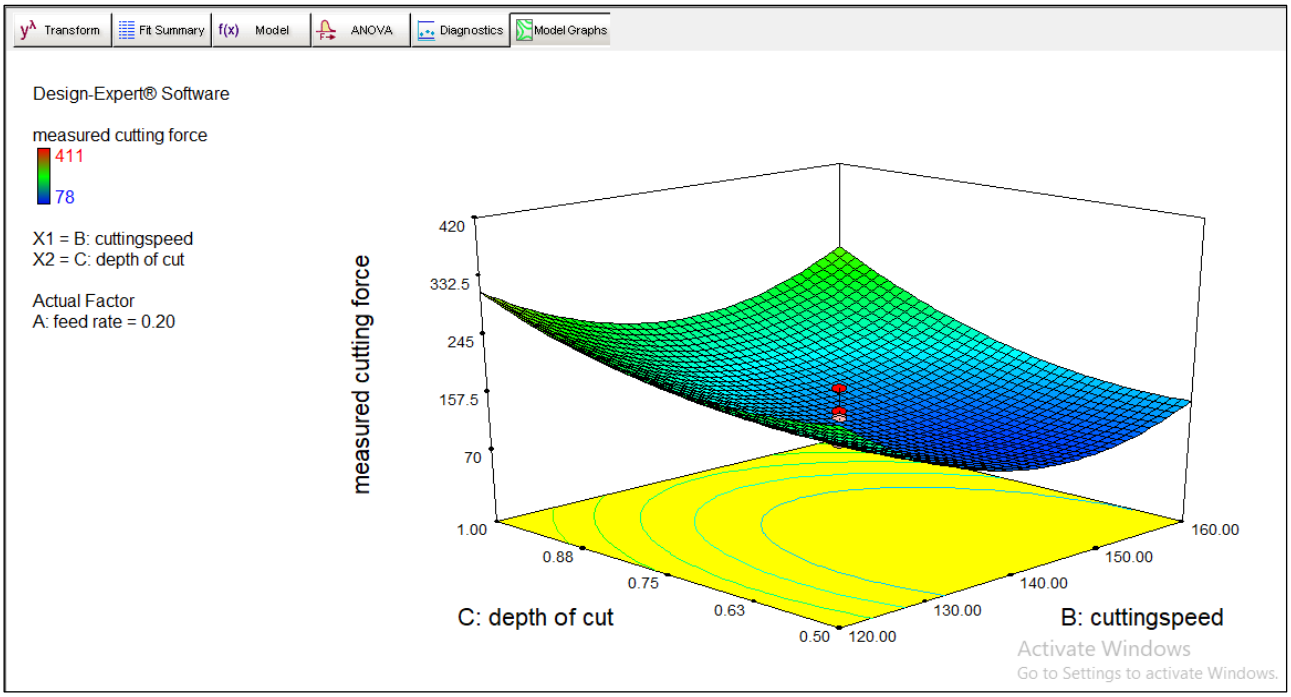

Figure 5: 3D Surface Plot for measured cutting force, depth of cut and cutting speed

The contour plots shows the relationship of the input variables (depth of cut, feed rate, and cutting speed) and the response variable (cutting force) .

Figure 6,7 and 8 displays the contour plots, based on the 3D Surface Plot.

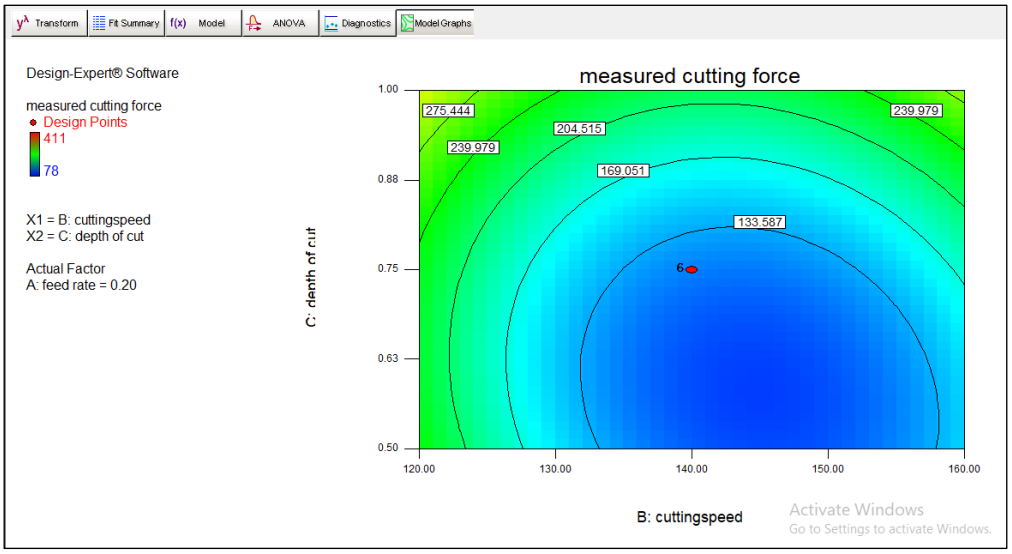

Figure 6: Contour plots measured cutting force, depth of cut and cutting speed

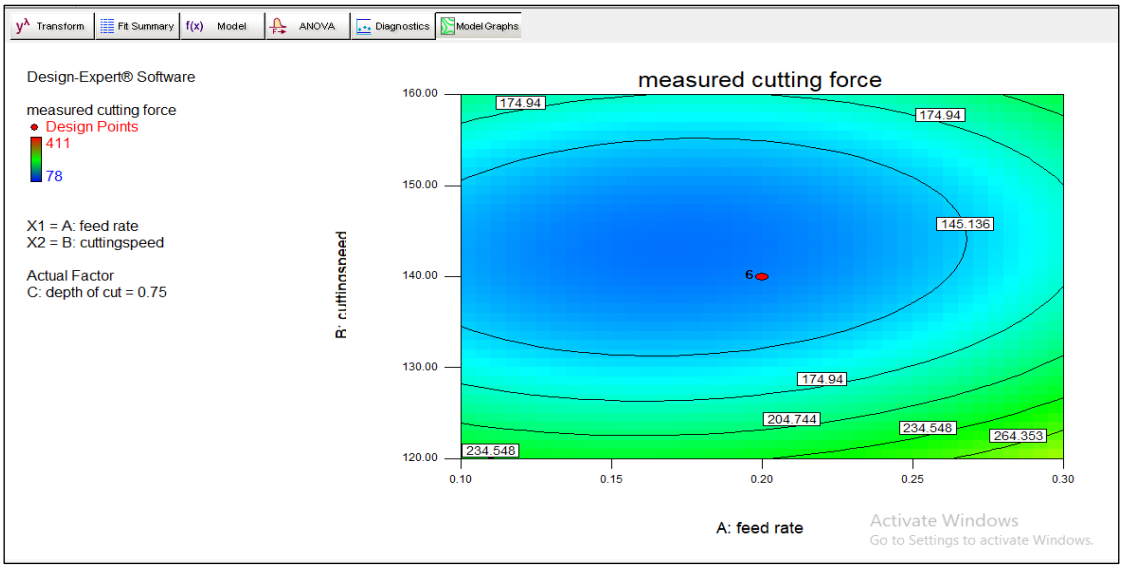

Figure 7: Contour plots measured Cutting force, cutting speed and feed rate

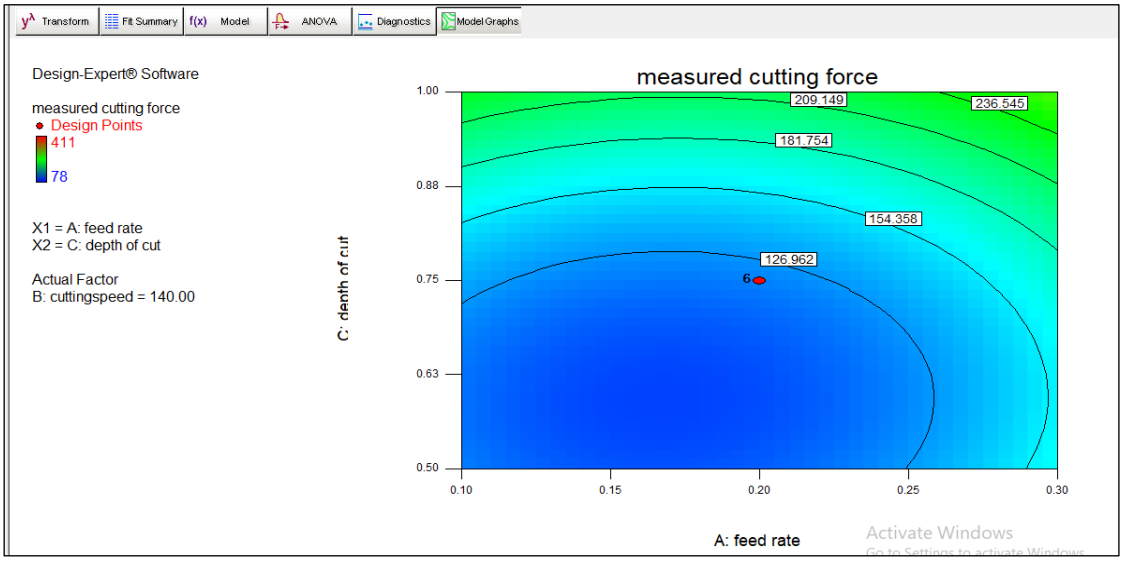

Figure 8: Contour plots measured Cutting force, depth of cut and feed rate

4.2 Modelling and Prediction using the ANN

The training, performance, and data division algorithms were configured as follows: Levenberg-Marquardt (Trainlm), mean squared error (MSE), and random (Dividerand). The neural network diagram used to forecast the cutting force responses is shown in Figure 9 while the trained network's performance curve is illustrated in Figure 10.

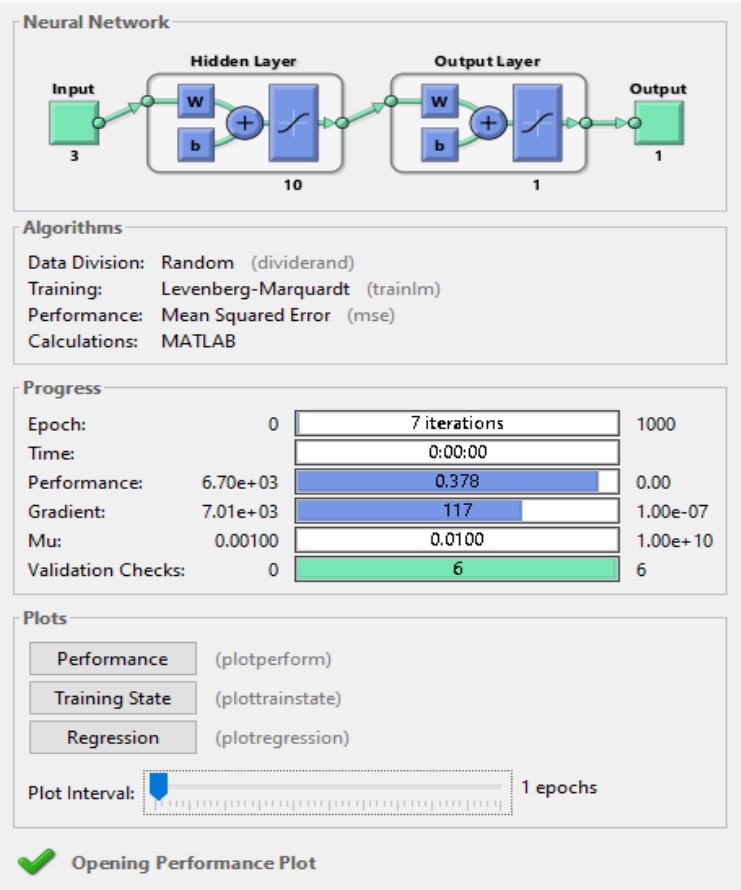

Figure 9: Network training diagram for predicting cutting force responses

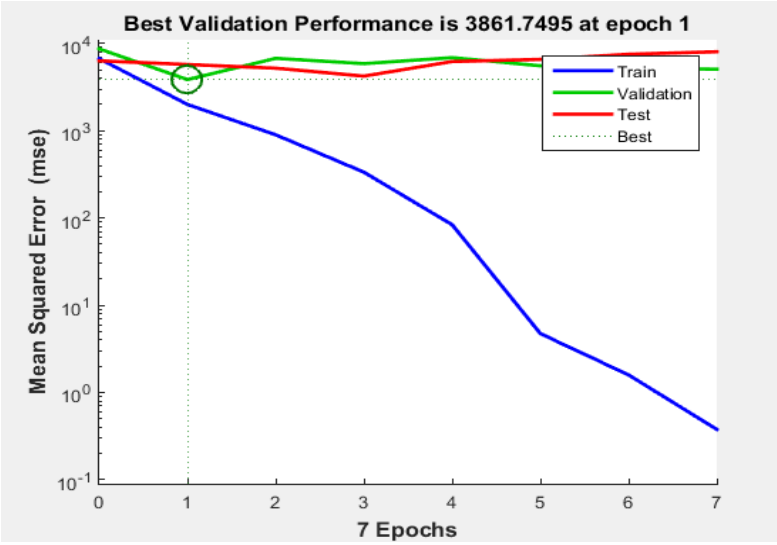

Figure 10: Performance curve for trained network to predicting cutting force responses

From Figure 9, the Network training diagram for predicting cutting force responses shows 7 iterations and 6 validation checks while Figure 10 the best validation performance at 3861.7495 at epoch 1. An epoch in MATLAB is equivalent to a whole training loop of an ANN. This indicates that one epoch has been reached when every vector in your training set has been used or processed by your training algorithm. As such, the training strategy employed determines the 'real-time duration' of a given epoch. Even though the iteration procedure required a total of 7 epochs, the best prediction for the cutting force responses was reached at epoch 1. The Neural network gradient plot for predicting cutting force response is described in Figure 11.

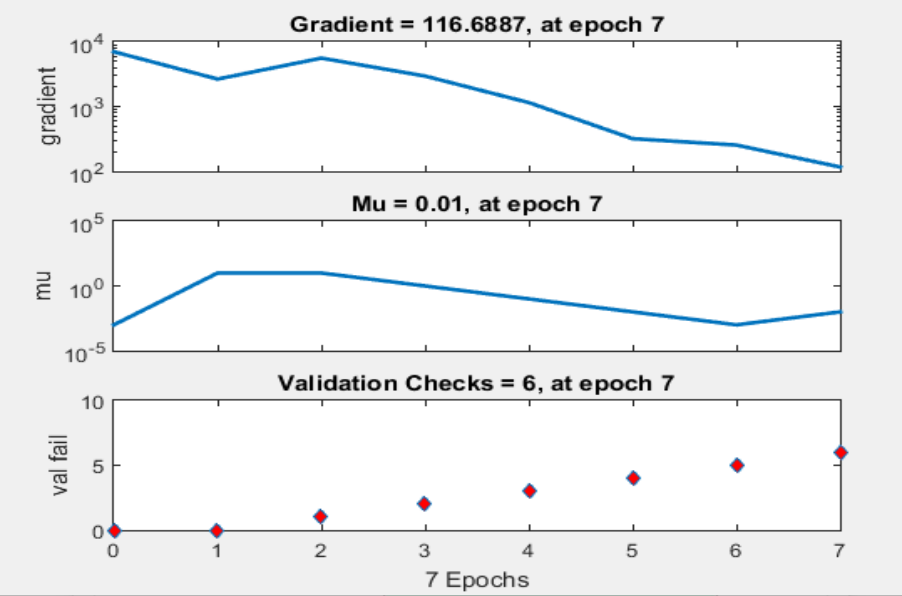

Figure 11: Neural network gradient plot for predicting cutting force responses

As one epoch denotes a single algorithm training cycle, from Figure 11, the number of epochs used up during training is at epoch 7. The dotted red lines for the validation checks showed that epoch 1 had the lowest failure rate, further indicating that the first epoch yielded the best forecast out of the seven epochs studied. The Regression plot of training, validation and testing for cutting force response is illustrated in Figure 12.

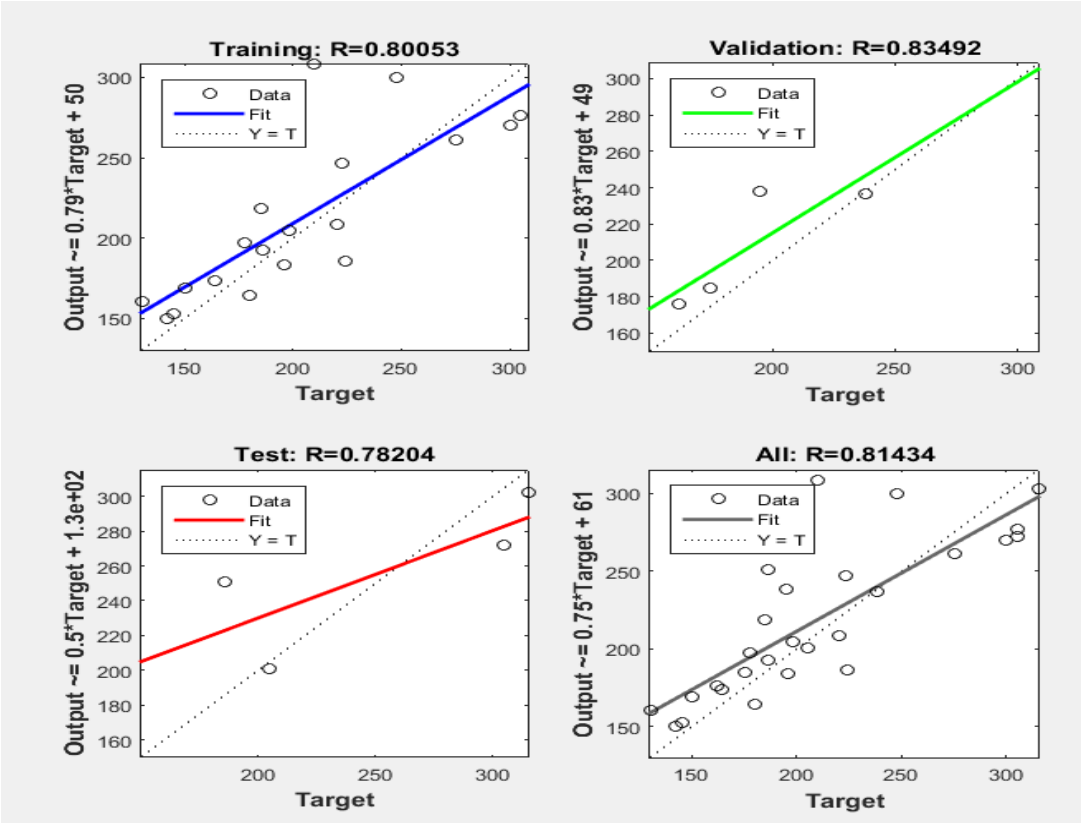

Figure 12: Regression plot of training, validation and testing for bead penetration responses.

Figure 15 describes the training, validation, and testing plots. The correlation coefficient (R) is seen to be more than 80%, indicating a reliable prediction for the cutting force.

5.1 CONCLUSION

The study has developed and applied two predictive expert techniques to model and predict the

cutting force by utilizing the RSM and ANN. The central component design (CCD) was used to design the experiment. The RSM model demonstrated a significant correlation between input parameters and cutting forces, as evidenced by its high coefficient of determination (R^2) of 0.9493. On the other hand, the ANN model, which was trained using 70% of the data and validated using 15% of the data, showed a little lower R^2 value of 0.81434, but it was still able to make accurate predictions. The RSM, in for this study is seen to be a better predictive expert system than the RSM. The results indicate that both RSM and ANN are useful instruments for dry drilling cutting force optimization, offering insights for increased productivity and efficiency in machining operations.

REFERENCES

1. Zhang, Y., & Xu, X. (2021). Machine learning cutting force, surface roughness, and tool life in high speed turning processes. *Manufacturing Letters*, *29*, 84-89.
2. Broderick, M., Turner, S., & Ridgway, K. (2021). Correlation between tool life and cutting force coefficient as the basis for a novel method in accelerated MWF performance assessment. *Procedia CIRP*, *101*, 366-369.
3. Lv, D., Wang, Y., & Yu, X. (2020). Effects of cutting edge radius on cutting force, tool wear, and life in milling of SUS-316L steel. *The International Journal of Advanced Manufacturing Technology*, *111*, 2833-2844.
4. Toubhans, B., Fromentin, G., Viprey, F., Karaouni, H., & Dorlin, T. (2020). Machinability of inconel 718 during turning: Cutting force model considering tool wear, influence on surface integrity. *Journal of Materials Processing Technology*, *285*, 116809.
5. Knápek, T., Dvořáčková, Š., & Váňa, M. (2023). The effect of clearance angle on tool life, cutting forces, surface roughness, and delamination during carbon-fiber-reinforced plastic milling. *Materials*, *16*(14), 5002.
6. Velan, M. V. G., Shree, M. S., & Muthuswamy, P. (2021). Effect of cutting parameters and high-pressure coolant on forces, surface roughness and tool life in turning AISI 1045 steel. *Materials Today: Proceedings*, *43*, 482-489.
7. Onozuka, H., Tayama, F., Huang, Y., & Inui, M. (2020). Cutting force model for power skiving of internal gear. *Journal of Manufacturing Processes*, *56*, 1277-1285.
8. Zhang, X., Zheng, G., Cheng, X., Li, Y., Li, L., & Liu, H. (2020). 2D fractal analysis of the cutting force and surface profile in turning of iron-based superalloy. *Measurement*, *151*, 107125.
9. Ali, S., Abdallah, S., & Pervaiz, S. (2022). Predicting cutting force and primary shear behavior in micro-textured tools assisted machining of AISI 630: Numerical modeling and taguchi analysis. *Micromachines*, *13*(1), 91.
10. Karpuschewski, B., Kundrák, J., Varga, G., Deszpoth, I., & Borysenko, D. (2018). Determination of specific cutting force components and exponents when applying high feed rates. *Procedia CIRP*, *77*, 30-33.
11. Imani, L., Rahmani Henzaki, A., Hamzeloo, R., & Davoodi, B. (2020). Modeling and optimizing of cutting force and surface roughness in milling process of Inconel 738 using hybrid ANN and GA. *Proceedings of the Institution of Mechanical Engineers, Part B: Journal of Engineering Manufacture*, *234*(5), 920-932.
12. Gupta, M. K., Korkmaz, M. E., Sarıkaya, M., Krolczyk, G. M., Günay, M., & Wojciechowski, S. (2022). Cutting forces and temperature measurements in cryogenic assisted turning of AA2024-T351 alloy: An experimentally validated simulation approach. *Measurement*, *188*, 110594.
13. Xiao, Q., Yang, Z., Zhang, Y., & Zheng, P. (2023). Adaptive optimal process control with actor-critic design for energy-efficient batch machining subject to time-varying tool wear. *Journal of Manufacturing Systems*, *67*, 80-96.
14. Jeyapandiarajan, P., & Xavior, A. (2019). Influence of cutting condition on machinability aspects of Inconel 718. *Journal of Engineering Research*, *7*(2).
15. Kuntoğlu, M., Aslan, A., Pimenov, D.Y., Usca, Ü.A., Salur, E., Gupta, M.K., Mikolajczyk, T., Giasin, K., Kapłonek, W. and Sharma, S., (2020). A review of indirect tool condition monitoring systems and decision-making methods in turning: Critical analysis and trends. *Sensors*, *21*(1), p.108